Proceedings of ICEF11
2011 Fall Technical Conference of the ASME Internal Combustion Engine Division
October 2-5, 2011, Morgantown, West Virginia, USA

ICEF2011-60028

AN OPTIMIZATION MODEL FOR PLUG-IN HYBRID ELECTIC VEHICLES*

Andreas A. Malikopoulos
Fuels, Engines, & Emissions Research Center
Energy & Transportation Science Division
Oak Ridge National Laboratory
Oak Ridge, Tennessee 37831,U.S.A

David E. Smith
Power Electronics & Elect. Pow. Syst. Res. Cent.
Energy & Transportation Science Division
Oak Ridge National Laboratory
Oak Ridge, Tennessee 37831,U.S.A

ABSTRACT

The necessity for environmentally conscious vehicle designs in conjunction with increasing concerns regarding U.S. dependency on foreign oil and climate change have induced significant investment towards enhancing the propulsion portfolio with new technologies. More recently, plug-in hybrid electric vehicles (PHEVs) have held great intuitive appeal and have attracted considerable attention. PHEVs have the potential to reduce petroleum consumption and greenhouse gas (GHG) emissions in the commercial transportation sector. They are especially appealing in situations where daily commuting is within a small amount of miles with excessive stop-and-go driving. The research effort outlined in this paper aims to investigate the implications of motor/generator and battery size on fuel economy and GHG emissions in a medium-duty PHEV. An optimization framework is developed and applied to two different parallel powertrain configurations, e.g., pre-transmission and post-transmission, to derive the optimal design with respect to motor/generator and battery size. A comparison between the conventional and PHEV configurations with equivalent size and performance under the same driving conditions is conducted thus allowing an assessment of the fuel economy and GHG emissions potential improvement. The post-transmission parallel configuration yields higher fuel economy and less GHG emissions compared to pre-transmission configuration partly attributable to the enhanced regenerative braking efficiency.

Keywords: plug-in hybrid electric vehicle, hybrid-electric vehicle, pre-transmission parallel configuration, post-transmission parallel configuration, design optimization, regression model, fuel economy, greenhouse gas emissions

1. INTRODUCTION

Medium-duty vehicles constitute a large market segment of the commercial transportation sector, and are also widely employed for military tactical operations. Improving the fuel efficiency on these vehicles has significant implications as fuel prices strain both the commercial transportation and military logistics support. Compression ignition engine technologies employed in medium and heavy-duty vehicles, such as fuel injection systems, variable geometry turbocharging (VGT), exhaust gas recirculation (EGR), and variable valve actuation (VVA), in conjunction with advanced control schemes have alleviated the traditional disadvantages of diesel engines, and facilitated their use in the transportation sector [1]. However, conventional internal combustion (IC) engine-driven powertrain systems have still several disadvantages that have an impact on fuel economy and emissions. In particular, IC engines are typically overdesigned by roughly 10 times to meet performance targets, such as acceleration and starting gradeability. Oversizing the engine moves the cruising operating point away from the optimal operation point while optimizing the engine over all speed and load operating ranges is impractical. Hybridization of conventional propulsion systems has been proved a viable approach towards decoupling the IC engine from the power demanded to cruise the vehicle.

Vehicle hybridization entails the existence of an alternative propulsion component in addition to the conventional engine-transmission-driveline powertrain, along with an energy storage device. Although hybridization creates many opportunities related to system architecture, the traditional classification includes two broad categories of hybrids, e.g., series and parallel, depending on whether there is a mechanical connection between the engine and the wheels. A variety of propulsion and energy storage system have been considered, such as electric, hydraulic, pneumatic or mechanical (flywheel). Having an alternative on-board storage device allows the regeneration and reuse of significant amounts of braking energy instead of dissipating it as heat. This feature is especially appealing in truck applications, where there is a lot of braking energy due to the large mass of the vehicles.

Hybrid electric vehicles (HEVs) have been shown the potential to achieve greater fuel economy compared to vehicles powered only by internal combustion engines (conventional vehicles) [2-4]. This capability is mainly attributed to: a) the potential for downsizing the engine; b) the potential of recovering energy during braking, and thus, recharging the energy storage unit; and c) the ability to minimize the operation of engine in inefficient brake specific fuel consumption (BSFC) regimes [5]. In addition, hybridization of conventional powertrain systems allows elimination of near idle engine operation, and thus, enabling in direct fuel economy enhancement [2, 3]. A typical HEV powertrain configuration consists of the fuel converter (engine), the electric machines (motor and generator), the energy storage system, e.g., battery, the torque coupler and the transmission. Depending on the driving mode, e.g., cruising or braking, either a positive or a negative torque is demanded from the engine. The power available from the electric machine is regulated by adjusting its torque such that it can be either positive or negative depending on the operating mode as designated by the power management control algorithm. In the motor mode, the electric machine contributes power to the driveline by drawing electrical energy from the energy storage unit. In the generator mode, the electric machine absorbs power from the driveline and charges the energy storage unit. In cruising, the power demanded from the powertrain is expressed by a positive amount of torque, given a fixed engine speed. In braking, the power is expressed by a negative torque. The electric machine (e.g., generator) absorbs the maximum possible amount as imposed by the generator and battery constraints. If a residual of braking amount remains, the friction brakes must handle this.

The automotive industry has recognized that widespread use of alternative hybrid powertrains is currently inevitable and many opportunities for substantial progress remain. The necessity for environmentally conscious vehicle designs in conjunction with stringent emission regulations has induced significant investment towards enhancing the propulsion portfolio with new technologies. More recently, plug-in hybrid electric vehicles (PHEVs) have held great intuitive appeal and have attracted considerable attention. PHEVs are hybrid vehicles with rechargeable batteries that can be restored to full charge by connecting a plug to an external electric wall socket. A PHEV shares the characteristics of both a HEV, having an electric motor and an internal combustion engine, and of an all-electric vehicle, also having a plug to connect to the electrical grid. It is especially appealing in situations where daily commuting is within a small amount of miles [6]. Studies have shown that approximately 60% of U.S. passenger vehicles travel less than 30 miles each day [7]. PHEVs have the potential to reduce petroleum consumption and greenhouse gas (GHG) emissions by means of sophisticated control schemes [8, 9]. Under the average mix of electricity sources in the U.S., PHEVs can be driven with lower operation cost and fewer greenhouse gas (GHG) emissions per mile when powered by electricity rather than by gasoline [10]. Most PHEVs on the road today are passenger cars, but there are also versions of commercial vehicles, utility trucks, buses, and military vehicles.

Various optimization approaches have been reported in the literature focusing on minimizing fuel consumption and emissions in hybrid vehicles with respect to component sizing and powertrain architecture. Earlier research efforts include the optimization study conducted by Triger *et al.* [11] to identify the optimal engine size in a hybrid electric vehicle. Aceves *et al.* [12] demonstrated the gain in fuel economy by optimizing two series hybrid concept vehicles, one operating with a stoichiometric engine and the other with a lean-burn engine. More [13] utilized a set of five linked spreadsheets to size powertrain components, based on continuous and peak power demand. Zoelch *et al*. [14] employed dynamic optimization to compute optimal engine, electric motor torque, and continuously variable transmission gear ratios for a parallel HEV. Assanis *et al.* [15] demonstrated an optimization framework for the design of a parallel hybrid-electric system for a mid-size passenger car linking a high fidelity engine model with the overall vehicle system. A modular simulation and design environment where optimization algorithms can be utilized to study a variety of hybrid powertrain configurations was presented by Fellini *et al* [16]. Recently, Shiau *et al*. [17] presented an optimization model integrating vehicle simulation polynomial metamodels, battery degradation data, and U.S. driving data; the proposed model identifies optimal vehicle designs and allocation of vehicles to drivers for minimum net life cycle cost, GHG emissions, and petroleum consumption under a range of scenarios.

Optimizing the design of a hybrid vehicle is tightly coupled with the power management control algorithm [18]. The latter determines the power split demanded by the driver between the thermal (engine) and electrical paths (electric machine and energy storage unit). Bumby *et al.* [19] used a direct search technique to obtain an optimal control by minimizing the energy path through the driving cycle with respect to torque split and gear ratio controllable variables. The optimized control was followed by parametric studies to optimize component size. Filipi *et al.* [20] proposed a novel methodology for the combined optimization of design and power management for a hydraulic hybrid Class VI truck. The

methodology establishes a sequential optimization framework suitable to yield a global optimal solution fulfilling a given vehicle's mission.

The research objective here is to investigate the impact of varying the size of two key components in a PHEV, e.g., the motor/generator and battery, on fuel economy and GHG emissions. This paper presents an optimization model that has implications for motor/generator and battery size in a medium-duty PHEV. A set of polynomial metamodel fits as function of the design variables is developed and utilized to formulate the problem analytically as well as to reduce the computational time. The optimization framework is applied to two different parallel powertrain configurations, e.g., pre-transmission and post-transmission, to derive the optimal design with respect to motor/generator and battery size. Finally, a comparison between the conventional and PHEV configurations with equivalent size and performance under the same driving conditions is conducted thus allowing an assessment of the fuel economy and GHG emissions potential improvement.

The remainder of the paper proceeds as follows. Section 2 presents the steps towards modeling the conventional and two PHEV parallel configurations into Autonomie. Section 3 develops a set of polynomial metamodel fits as function of the design variables, i.e., motor/generator and battery size, and introduces the optimization framework. Simulation results are presented in Section 4. Conclusions are drawn in Section 5.

TABLE 1
VEHICLE SPECIFICATIONS

	Description	Characteristics
Vehicle	Mass	33,000 lbs
	Body Length	34'2''
	Frontal Area	68 ft^2
	Coefficient of Drag	0.65
Engine	Configuration	V8
	Displacement	6.4L
	HP	230
	Torque	230 lb-ft
	Rated Speed	2,800 RPM
	Operating Torque Speed	1,400-1,800 RPM
	Dry Weight	1,225 lbs
Transmission	1st Gear Ratio	3.51
	2nd Gear Ratio	1.9
	3rd Gear Ratio	1.44
	4th Gear Ratio	1
	5th Gear Ratio	0.74
	6th Gear Ratio	0.64
	Reverse	5.09
Torque Converter	TC Stall Torque Ratio	1.91
Starter	Power	25 kW

2. PROPULSION SYSTEM MODELING

For the evaluation of various performance vehicle indices required for our optimization study, we employ Autonomie [21]. Autonomie is a Matlab/Simulink simulation package for powertrain and vehicle model development, developed by Argonne National Laboratory. With a variety of existing forward-looking powertrain and vehicle models, Autonomie can support the evaluation of new technologies for improving fuel economy through virtual design and analysis in a math-based simulation environment.

The two PHEV parallel configuration models are subjected to a specific duty cycle representative of typical operation; for this particular medium duty vehicle the Japanese JE-05 driving cycle, illustrated in Figure 1, is selected. To utilize the full energy storage potential of the energy storage system, the vehicle models are run over nine consecutive JE-05 cycles. Consequently, both full charge-depleting (CD) and charge-sustaining (CS) operation are achieved.

Three basic powertrain configurations are analyzed as part of this study, and are summarized below. For each respective powertrain variant, certain components are kept constant. Table 1 outlines all of the common components present in each powertrain configuration, including the conventional vehicle. Table 2 outlines common powertrain components utilized only for the pre- and post-transmission parallel PHEV architectures.

We adopt a blended supervisor control strategy that utilizes a mix of the electric motor and engine to power the vehicle in CD mode. For the purposes of all the PHEV simulations, the state of charge (SOC) of the vehicle is allowed to fluctuate with a delta SOC of 60% (80% initial SOC depleting to 20% SOC). Certain constraints are placed on the control strategy for the desired operation of this vehicle, e.g., the powertrain must operate as an all-electric vehicle below vehicle speeds of 25 MPH during CD operation, and the engine must turn on at vehicle speeds greater than 45 mph for drivability reasons.

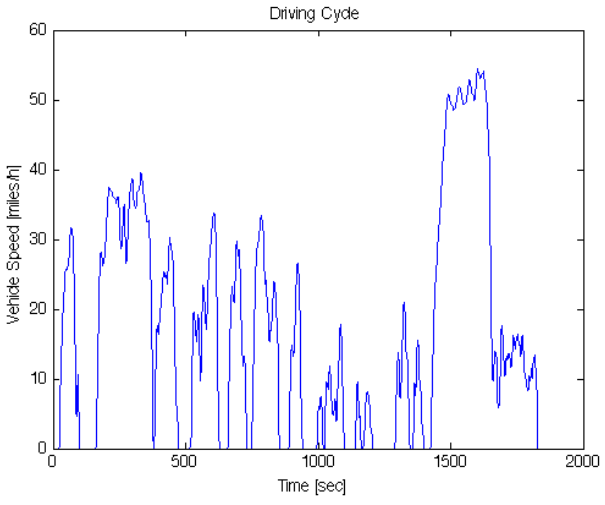

Figure 1. Japanese driving cycle.

TABLE 2
PLUG-IN HYBRID-ELECTRIC VEHICLE COMPONENTS SPECIFICATIONS

	Description	Characteristics
Battery	Nominal Voltage	425 V
	Charge	1/5C
	Discharge	10/20C
	Number of cells in series per module	118
	Number of cells in parallel per module	1
Motor/ Generator	Range of continuous power used	60-120 kW
Final Drive	Ratio	5.57
Torque Converter	TC Stall Torque Ratio	1.91
Reduction Gear	Ratio	2.13

Conventional configuration. A conventional powertrain, shown in Figure 2, is implemented to serve as a point of reference. The conventional vehicle features a basic two-wheel drive configuration with automatic transmission and torque converter. Standard transmission shift schedules are employed based upon accelerator pedal position (driver demand) and current vehicle speed.

Pre-transmission parallel configuration. The pre-transmission parallel configuration, illustrated in Figure 3, builds upon the conventional architecture by adding a high voltage traction drive and energy storage system at the interface of the engine. In this implementation, the torque converter is replaced by a clutch, and the motor/generator is used for speed matching during shifts. Thus, this configuration resembles an operation with automated manual transmission. One potential advantage of this architecture over the post-transmission variant is that vehicle idle charging is possible. If this vehicle is subjected to long periods of idle, then turning the engine on and charging can easily replenish the SOC of the energy storage system.

Post-transmission parallel configuration. The post-transmission parallel configuration, shown in Figure 4, builds upon the conventional architecture by coupling a high voltage traction drive and energy storage system between the transmission and final drive. The latter is necessary to full realize the operating envelope of the traction motor such that the performance of this variant is not compromised over the prescribed drive cycle. During all electric operation, the transmission is shifted into neutral such that drag torque from the engine is avoided. One benefit of this architecture over the pre-transmission variant is regenerative braking efficiency is maximized due to physical location of the traction motor. There are fewer to no spinning losses through the transmission in this case.

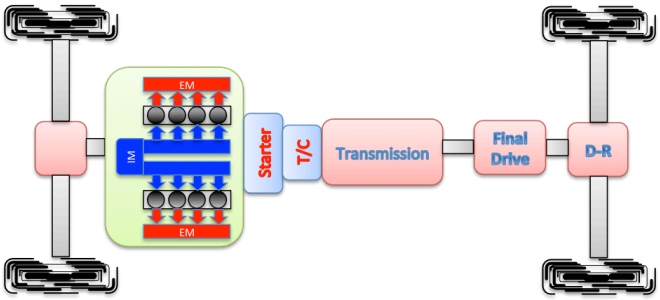

Figure 2. Conventional powertrain configuration.

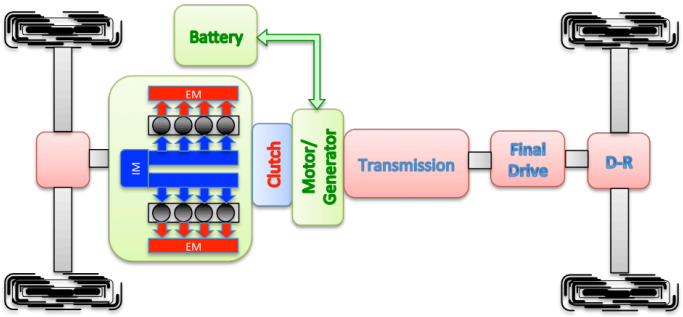

Figure 3. PHEV pre-transmission parallel powertrain configuration.

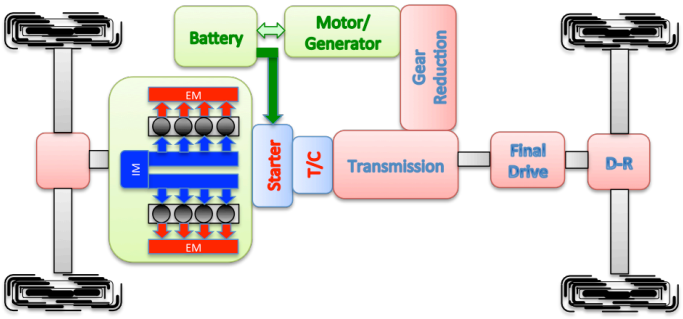

Figure 4. PHEV post-transmission parallel powertrain configuration.

It is important to note that since the PHEV variants of the standard powertrain configuration retain all of the baseline components (e.g., transmission, final drive, engine, chassis, wheels), it is expected that during highway operation the fuel efficiency of the PHEV will most likely be slightly less than the conventional vehicle due to the mass penalty imposed by the addition of the high voltage traction components.

3. OPTIMIZATION MODEL

To formulate the optimization problem analytically and reduce computation time, a set of polynomial metamodels are constructed to reflect the responses produced by changes in the design variables, e.g., motor/generator and battery size. Metamodel is a "model of model," which is used to approximate a usually expensive analysis or simulation process; metamodeling refers to the techniques and procedures to construct such a model [22]. In our optimization framework, a set of polynomial metamodels is used to express the objective function and the constraints in the problem formulation. In particular, fuel economy, GHG emissions, 0-30 mph and 0-60 mph acceleration time are evaluated though simulation in Autonomie over a grid of values for motor/generator and battery sizes. Then multivariate polynomial functions are fit to the data employing least squares.

3.1 Regression model

The least-squares method is a fundamental approach for parameter estimation. If the model has the property of being linear in the parameters then the least-squares estimate can be calculated analytically [23]. We assume that the model we wish to identify is in the form

$$\hat{y}(i) = \varphi_1(i)\cdot\alpha_1 + \varphi_2(i)\cdot\alpha_2 + ... + \varphi_n(i)\cdot\alpha_n , \quad (1)$$

where $i = 1,2,...,n, n \in \aleph$, indexes the number of simulation data points, $\hat{y}$ is the output of the model, $\alpha_1,\alpha_2,...,\alpha_n$ are the parameters of the model to be determined, and $\varphi_1,\varphi_2,...,\varphi_n$ are known functions that may depend on other known variables. The model in Eq. (1) can be written in the vector form as follows

$$\hat{y}(i) = \boldsymbol{\varphi}^T(i)\cdot\boldsymbol{\alpha} , \quad (2)$$

where $\boldsymbol{\varphi}^T(i) = \left[\varphi_1(i)\ \ \varphi_2(i)\ ...\ \ \varphi_n(i)\right]$ and $\boldsymbol{\alpha} = \left[\alpha_1\ \ \alpha_2\ ...\ \ \alpha_m\right]^T$. The model in Eq. (1) is the *regression model* and the functions $\varphi_i, i = 1,2,...,n$, are called the *regression variables*. The simulation data points derived from Autonomie correspond to pairs of the measured and regression variables $\left\{(y(i),\boldsymbol{\varphi}(i)), i = 1,2,...,n, n \in \aleph\right\}$. The problem is formulated as to minimize the following least squares cost function

$$R(\alpha,n) = \frac{1}{2}\sum_{i=1}^{n}\left[y(i) - \hat{y}(i)\right]^2 = \frac{1}{2}\sum_{i=1}^{n}\left[y(i) - \boldsymbol{\varphi}^T(i)\cdot\boldsymbol{\alpha}\right]^2 , \quad (3)$$

with respect to the parameters of the model $\alpha_1,\alpha_2,...,\alpha_n$. The measured variable y is linear in parameters α_i and the cost function is quadratic. Consequently, the problem admits an analytical solution. Let $\mathbf{Y}$ and $\hat{\mathbf{Y}}$ be the vector of the measured variables and output of the model respectively

$$\mathbf{Y} = \left[y(1), y(2), ..., y(n)\right]^T , \text{ and} \quad (4)$$

$$\hat{\mathbf{Y}} = \left[\hat{y}(1), \hat{y}(2), ..., \hat{y}(n)\right]^T , \quad (5)$$

and let $\mathbf{E}$ be the vector of the error $e(i)$ between the measured variable and output of the model

$$\mathbf{E} = \left[e(1), e(2), ..., e(n)\right]^T , \quad (6)$$

where $e(i) = y(i) - \hat{y}(i) = y(i) - \boldsymbol{\varphi}^T(i)\cdot\boldsymbol{\alpha}$. Substituting Eq. (6) to Eq. (3) the cost function can be written as

$$R(\alpha,n) = \frac{1}{2}\sum_{i=1}^{n} e(i)^2 = \frac{1}{2}\left\|\mathbf{E}\right\|^2 . \quad (7)$$

Our objective is to derive the vector of the model parameters $\boldsymbol{\alpha}$ that make the error be equal to zero, that is

$$\mathbf{E} = \mathbf{Y} - \hat{\mathbf{Y}} = \mathbf{Y} - \boldsymbol{\Phi}\cdot\boldsymbol{\alpha} = 0 , \quad (8)$$

where $\boldsymbol{\Phi}(n) = \left[\boldsymbol{\varphi}^T(1)\ \ \boldsymbol{\varphi}^T(2)\ ...\ \ \boldsymbol{\varphi}^T(n)\right]^T$. Consequently, the solution of the least squares problem is given by solving Eq. (8), namely

$$\begin{gathered}\mathbf{Y} = \boldsymbol{\Phi}\cdot\boldsymbol{\alpha} \Leftrightarrow \\ \boldsymbol{\Phi}^T\cdot\mathbf{Y} = \boldsymbol{\Phi}^T\cdot\boldsymbol{\Phi}\cdot\boldsymbol{\alpha} \Leftrightarrow \\ \left(\boldsymbol{\Phi}^T\cdot\boldsymbol{\Phi}\right)^{-1}\cdot\boldsymbol{\Phi}^T\cdot\mathbf{Y} = \left(\boldsymbol{\Phi}^T\cdot\boldsymbol{\Phi}\right)^{-1}\cdot\left(\boldsymbol{\Phi}^T\cdot\boldsymbol{\Phi}\right)\cdot\boldsymbol{\alpha} \Leftrightarrow \\ \boldsymbol{\alpha} = \left(\boldsymbol{\Phi}^T\cdot\boldsymbol{\Phi}\right)^{-1}\cdot\boldsymbol{\Phi}^T\cdot\mathbf{Y} . \end{gathered} \quad (9)$$

If the matrix $\boldsymbol{\Phi}^T\cdot\boldsymbol{\Phi}$ is nonsingular, then the solution of Eq. (9) is a unique minimum for the least squares problem [23].

3.2 Optimization objective function and constraints

In our optimization problem formulation, the vector of the design variables $\mathbf{x}$ consists of the motor/generator size x_1, and the battery size x_2. The set of polynomial metamodels is a function of the vector $\mathbf{x}$. For fuel economy, $f_{fuel\ \text{economy}}$ (mpg), a cubic fitting function of the form

TABLE 3
POLYNOMIAL COEFFICIENTS OF THE PHEV PRE-TRANSMISSION PARALLEL CONFIGURATION METAMODELS

	$f_{fuel\ \text{economy}}$	f_{CO_2}	t_{0-30}	t_{0-60}
a_1	0.0000	0.0022	0.0002	0.0000
a_2	-0.0777	2.3637	-0.0106	0.0283
a_3	0.0002	-0.0003	0.0000	0.0000
a_4	0.0026	-0.0184	0.0001	-0.0002
a_5	-0.0020	0.3194	-0.0015	0.0038
a_6	1.5362	-1.3773	-0.1382	-0.1966
a_7	-0.0717	-36.3434	0.2987	-0.1512
a_8	0.4407	236.7877	24.0720	48.0366
a_9	-7.5871			
a_{10}	16.3026			
$\|r\|$	0.59	3.52	1.51	2.53

TABLE 4
POLYNOMIAL COEFFICIENTS OF THE PHEV POST-TRANSMISSION PARALLEL CONFIGURATION METAMODELS

	$f_{fuel\ \text{economy}}$	f_{CO_2}	t_{0-30}	t_{0-60}
a_1	-0.0002	0.0021	0.0001	0.0000
a_2	-0.0004	2.4002	0.0132	-0.0089
a_3	0.0002	-0.0003	0.0000	0.0000
a_4	0.0078	-0.0180	-0.0001	0.0001
a_5	0.0428	0.2971	-0.0008	-0.0029
a_6	-0.8028	-1.2047	-0.1580	-0.2047
a_7	-0.1314	-36.2471	0.0949	0.5573
a_8	-3.3305	227.4291	28.0850	487277
a_9	13.4367			
a_{10}	69.6121			
$\|r\|$	2.03	7.20	1.87	2.86

$$f(x_1,x_2)=\alpha_1x_1^3+\alpha_2x_2^3+\alpha_3x_1^2x_2+\alpha_4x_1x_2^2+ \\ +\alpha_5x_1^2+\alpha_6x_2^2+\alpha_7x_1x_2+\alpha_8x_1+\alpha_9x_2+a_{10}\,, \quad (10)$$

provides an appropriate fitting to the discrete simulation data points [22]. A higher order polynomial metamodel appears to overfit the simulation data points whereas a lower order polynomial is not adequate. For the following PHEV performance indices: (a) GHG emissions, f_{CO_2} (kg-CO_2), (b) 0-30 mph acceleration time, t_{0-30} (sec), and (c) 0-60 mph acceleration time, t_{0-60} (sec), a quadratic fitting function of the form

$$f(x_1,x_2)=\alpha_1x_1^2+\alpha_2x_2^2+\alpha_3x_1^2x_2+\alpha_4x_1x_2^2+ \\ +\alpha_5x_1x_2+\alpha_6x_1+\alpha_7x_2+\alpha_8\,, \quad (11)$$

can fit the discrete simulation data points satisfactory [22]. A higher order polynomial metamodel overfits the simulation data points for these performance indices.

Eqs. (10) and (11) are the regression models employed for each of the output values to fit a set of discrete simulation data points over a grid of values for the design variables x_1 and x_2. The polynomial coefficients of these models are derived utilizing least squares. The vector of known functions, $\boldsymbol{\varphi}^T$, in Eq. (10) is

$$\boldsymbol{\varphi}^T(i)=[x_1^3(i)\quad x_2^3(i)\quad x_1^2(i)\cdot x_2(i)\quad x_1(i)\cdot x_2^2(i) \\ x_1^2(i)\quad x_2^2(i)\quad x_1(i)\cdot x_2(i)\quad x_1^2(i)\quad x_2^2(i)\quad 1\big]\,, \quad (12)$$

and the vector of known functions, $\boldsymbol{\varphi}^T$, in Eq. (11) is

$$\boldsymbol{\varphi}^T(i)=[x_1^2(i)\quad x_2^2(i)\quad x_1^2(i)\cdot x_2(i)\quad x_1(i)\cdot x_2^2(i) \\ x_1(i)\cdot x_2(i)\quad x_1^2(i)\quad x_2^2(i)\quad 1\big]\,. \quad (13)$$

The range of values for the motor/generator size, x_1, used to derive the simulation data points in continuous power is $x_1=\{60,80,100,120\}$ kW. Similarly, the range of values for the battery size in number of modules is $x_2=\{6,7,8,9,10\}$, each of which includes 118 cells in series and 1 cell in parallel. As a result, the simulation data set is created over a grid of 20 different inputs, i.e., $i=1,2,...,20$.

Fuel consumption. The amount of fuel consumed by each vehicle for the nine consecutive JE-05 driving cycles is computed directly by Autonomie. Autonomie also provide the values of fuel economy, $f_{fuel\ \text{economy}}$, in miles per gallon.

Greenhouse gas emissions. The average GHG emissions, f_{CO_2}, in kg CO_2 (kg-CO_2) for the nine consecutive JE-05 cycles is associated with the amount of CO_2 corresponding to diesel and electricity portion. Consequently, given the fuel efficiency, η_{fuel}, (mpg) and electricity efficiency, η_E, (miles/kWh) derived from simulation in Autonomie, the average GHG emissions is computed by the following equation

$$f_{CO_2}=s\cdot\left(\frac{N_{CO_2}^D}{\eta_{fuel}}+\frac{N_{CO_2}^E}{\eta_E}\cdot\frac{1}{\eta_{BC}}\right), \quad (14)$$

where s = 77 miles is the distance driven by the vehicle over the nine consecutive JE-05 driving cycles, $N_{CO_2}^D$ = 10.1 kg-CO_2/gal for diesel life cycle emissions [24], $N_{CO_2}^E$ =0.752 kg-CO_2/kWh

for electricity emissions [25, 26], and η_{BC}=88% for battery charging efficiency [26].

Acceleration performance metrics. For the 0-30 mph and 0-60 mph acceleration time, t_{0-30}(sec) and t_{0-60}(sec), we perform simulated tests in CS mode in Autonomie.

Utilizing the discrete simulation data points from Autonomie derived over the input grid described above, we compute the polynomial fitting coefficients, $\boldsymbol{\alpha}$, for each regression model, i.e., $f_{fuel\ economy}$, f_{CO_2}, t_{0-30}, and t_{0-60} by solving Eq. (9) using Eqs. (12) and (13) respectively. The resulting values of polynomial coefficients are listed in Tables 3 and 4. To evaluate the polynomial fitting with the discrete simulation data points the norm of residuals is employed given by

$$\|r\| = \left(\sum_{i=1}^{n} \left(y(i) - \hat{y}(i) \right)^2 \right)^{1/2}. \qquad (15)$$

The values of the norm of residuals for each regression model are listed in Tables 3 and 4.

3.3 Optimization problem formulation

The optimization framework established here aims to determine the impact of the vector of the design variables, $\mathbf{x}$, consisting of the motor/generator size x_1, and battery size x_2, on both fuel economy and GHG emissions. Moreover, the optimization study intends to identify which one of the two PHEV configurations is more efficient in terms of fuel economy and GHG emissions.

For each PHEV configuration, an optimization problem is formulated; the objective is to maximize fuel economy and minimize GHG emissions with respect to the vector of the design variables, $\mathbf{x}$, subject to the acceleration performance metrics. The mathematical problem consists of the following multi-objective function and constraints

$$\min_{\mathbf{x}} \left(w_1 \cdot \frac{1}{f_{fuel\ \text{economy}}(\mathbf{x})} + w_2 \cdot f_{CO_2}(\mathbf{x}) \right) \qquad (16)$$

$$\text{subject to } t_{0-30} \le 15\,\text{sec}$$
$$t_{0-60} \le 55\,\text{sec},$$

where w_1=0.5 and w_2=0.5 are the weighting factors of the objective function.

Furthermore, a comparison of the conventional and the optimized PHEV parallel configurations over the Urban Dynamometer Driving Schedule (UDDS) and the Japanese JE-05 driving cycle is conducted thus allowing an assessment of the fuel economy and GHG emissions potential improvement.

4. SIMULATION RESULTS

The impact of varying the motor/generator and battery size on fuel economy in PHEV pre-transmission and post-transmission parallel configurations is illustrated in Figure 5 and Figure 6 respectively. Increasing the battery size has a significant repercussion in fuel economy, partly attributable to the additional amount of electricity from grid that can be stored and utilized to power the vehicle. The motor/generator size, on the other hand, has significant contributions to fuel economy only in conjunction with a large battery size. The combination of a large motor/generator and battery size yield an enhanced capability to recover energy during brake regeneration. The latter is more apparent in the PHEV post-transmission configuration where fuel economy is noticeably improved.

Increasing the battery size has some interesting implications for GHG emissions. For small motor/generator, increasing the number of modules in the battery is not beneficial for GHG emissions. On the contrary, a moderate number of modules around 7 seem to be the optimal battery size for both configurations as illustrated in Figure 7 and Figure 8. For a large motor/generator size the impact of a large battery is quite different for the pre- and post- transmission configurations. In particular, for the PHEV pre-transmission configuration GHG emissions are minimal for a combination of a 120 kW motor/generator size with a 6-module battery. For the PHEV post-transmission configuration, on the other hand, a 120 kW motor/generator size a battery with 10 modules seems to be the optimal solution for GHG emissions.

Although by increasing the battery size the contribution in GHG from electricity grid is also increased, Eq. (14), this is compensated by the enhanced capability of post-transmission configuration to store energy from brake regeneration.

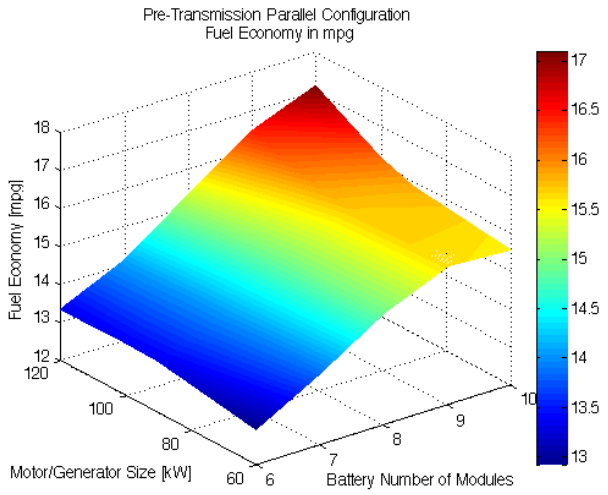

Figure 5. Fuel economy variation in PHEV pre-transmission.

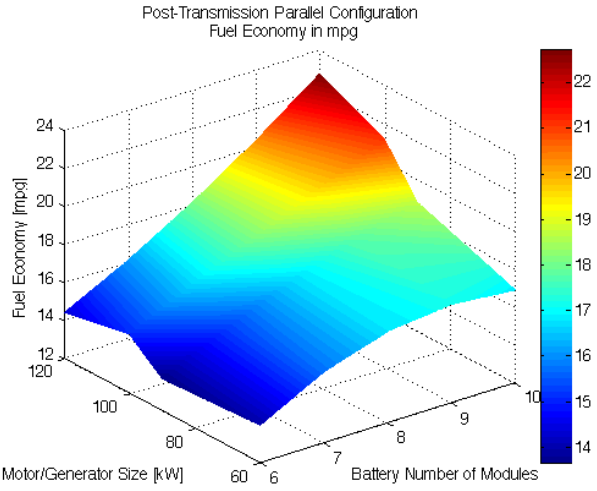

Figure 6. Fuel economy variation in PHEV post-transmission.

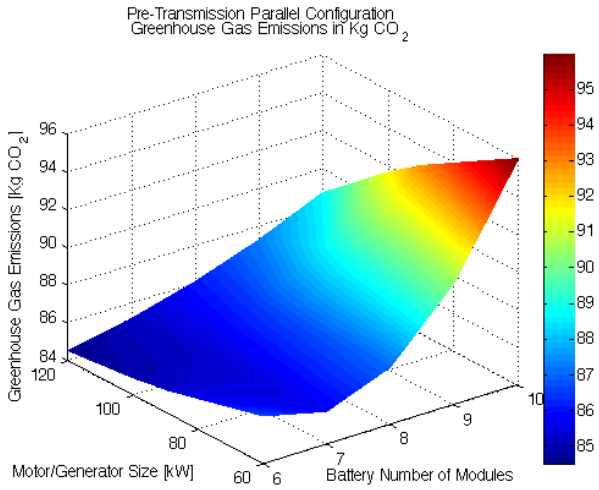

Figure 7. GHG emissions in PHEV pre-transmission.

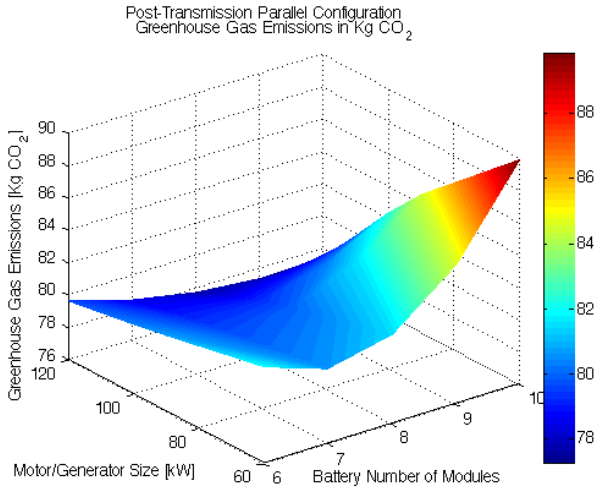

Figure 8. GHG emissions in PHEV post-transmission.

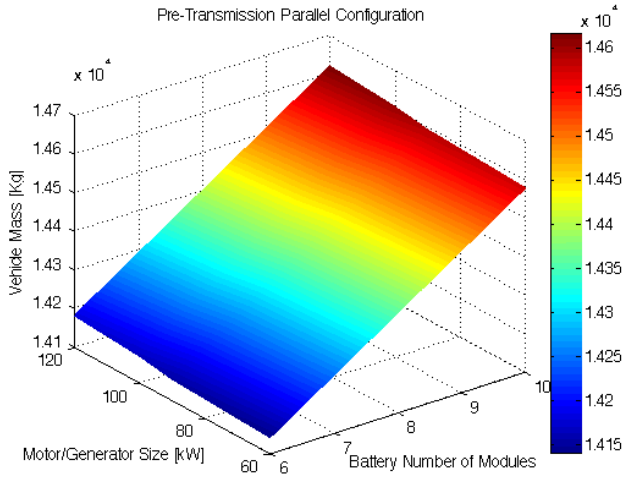

Figure 9. Vehicle mass for the PHEV pre-transmission.

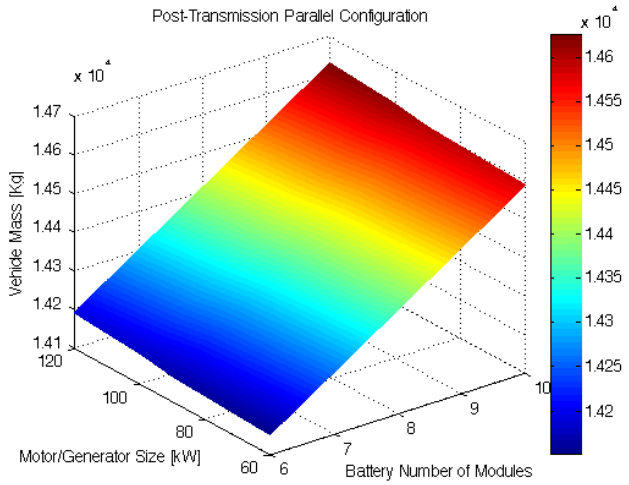

Figure 10. Vehicle mass for the PHEV post-transmission.

The multi-objective optimization problem formulated in Eq. (16) has an apparent visual solution for the PHEV post-transmission configuration, as shown in Figure 6 and Figure 8; namely, the optimal solution for both fuel economy and GHG emissions is a 120 kW motor/generator size with a 10-module battery. For the PHEV pre-transmission configuration it seems that there is trade-off between fuel economy and GHG emissions, shown in Figure 5 and Figure 7, for large motor/generator and battery size. However, solving the problem analytically, a 120 kW motor/generator size with a 10-module battery is the optimal solution in this case as well. Although the 10-module battery increases GHG emissions for a 120 kW motor/generator size, the contribution of fuel economy in the multi-objective function, Eq. (16), is substantial. Certainly, different weighting factors between fuel economy and emission in the Eq. (16) would yield different results.

Increasing the motor/generator and battery size has, as might be expected, an impact on the vehicle mass as depicted in

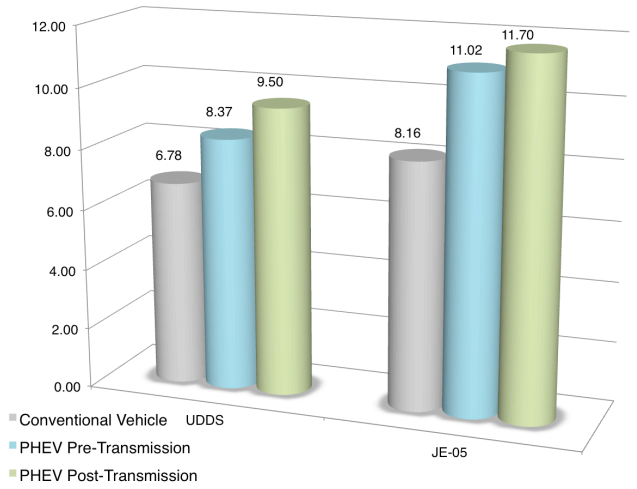

Figure 11. Fuel economy in mpg over UDDS and JE-05 driving cycles (PHEVs in CS mode).

Figure 9 and Figure 10, with significant implications on both packaging and cost. However, the consideration of packaging and cost repercussions is beyond the scope of this paper.

A comparison of the conventional and the optimized PHEV parallel configurations over two driving cycles, i.e., the Urban Dynamometer Driving Schedule (UDDS) and the Japanese JE-05 cycle, is conducted thus allowing an assessment of the fuel economy and GHG emissions potential improvement. The PHEV post-transmission parallel configuration yields higher fuel economy and less GHG emissions in kg CO_2 over the two driving cycles compared to both pre-transmission and conventional vehicles as illustrated in Figure 11 and Figure 12.

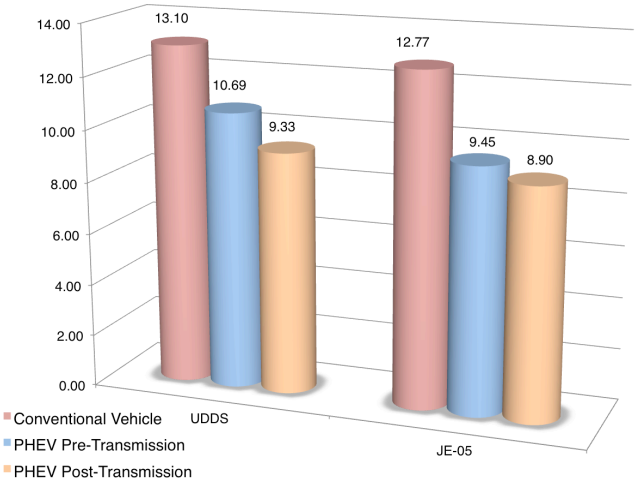

Figure 12. GHG emission in Kg CO_2 on CS mode over UDDS and JE-05 driving cycles (PHEVs in CS mode).

The important advantage of this architecture over the pre-transmission variant is that regenerative braking efficiency is maximized due to physical location of the traction motor.

5. CONCLUDING REMARKS

This paper presented an optimization framework to investigate the implications of motor/generator and battery size on fuel economy and GHG emissions in a medium-duty PHEV. An optimization model was developed and applied to two different parallel powertrain configurations, e.g., pre-transmission and post-transmission, to derive the optimal design with respect to motor/generator and battery size. A comparison between the conventional and PHEV configurations with equivalent size and performance under the same driving conditions was conducted thus allowing an assessment of the fuel economy and GHG emissions potential improvement. The post-transmission parallel configuration yields higher fuel economy and less GHG emissions compared to pre-transmission configuration partly attributable to the enhanced regenerative braking efficiency.

The research effort outlined in this paper aims to facilitate better understanding of the benefits in fuel economy and GHG emissions with respect to motor/generator and battery size. For PHEV powertrain configurations consistent to those study here, our results imply that the size of these components is a critical design variable. Future research should investigate the implications of power management control algorithms in conjunction with the optimization of the design variables in a PHEV. Optimizing the design of a PHEV is tightly coupled with the power management controller, and a simultaneous consideration of both may yield more opportunities for substantial improvements in fuel economy and GHG emissions.

ACKNOWLEDGMENTS

This research was supported by the U. S. Department of Energy, Office of Energy Efficiency and Renewable Energy, Vehicle Technologies Program, under contract DE-AC05-00OR22725 with UT-Battelle, LLC. This support is gratefully acknowledged.

REFERENCES

[1] A. A. Malikopoulos, D. N. Assanis, and P. Y. Papalambros, "Real-Time Self-Learning Optimization of Diesel Engine Calibration," *ASME J. Eng. Gas Turbines Power,* vol. 131, p. 022803(7), 2009.

[2] A. Sciarretta and L. Guzzella, "Control of Hybrid Electric Vehicles," *IEEE Control Systems Magazine,* vol. 27, pp. 60-70, 2007.

[3] A. Sciarretta, M. Back, and L. Guzzella, "Optimal Control of Parallel Hybrid Electric Vehicles," *IEEE Transactions on Control Systems Technology,* vol. 12, pp. 352-363, 2004.

[4] N. J. Schouten, M. A. Salman, and N. A. Kheir, "Energy Management Strategies for Parallel Hybrid Vehicles Using Fuzzy Logic," *Control Engineering Practice,* vol. 11, pp. 171-177, 2003.
[5] A. A. Malikopoulos, Z. S. Filipi, and D. N. Assanis, "Simulation of an Integrated Starter Alternator (ISA) System for the HMMWV," Proceedings of *SAE 2006 World Congress and Exhibition, SAE 2006-01-0442*, Detroit, Michigan, 2006.
[6] Q. Gong, Y. Li, and Z.-R. Peng, "Trip-based Optimal Power Management of Plug-in Hybrid Electric Vehicles," *IEEE Transactions on Vehicular Technology,* vol. 57, pp. 3393-3401, 2008.
[7] L. Johannesson, M. Asbogard, and B. Egardt, "Assessing the potential of predictive control for hybrid vehicle powertrains using stochastic dynamic programming," *IEEE Transactions on Intelligent Transportation Systems,* vol. 8, pp. 71-83, 2007.
[8] D. E. Smith, "Plug-In Hybrid Electric Vehicle Emissions Impacts on Control Strategy and Fuel Economy," Ph.D. Dissertation, Department of Mechanical Engineering, University of Tennessee, Knoxville, TN, 2009.
[9] D. E. Smith, H. Lohse-Busch, and D. K. Irick, "A Preliminary Investigation Into the Mitigation of Plug-in Hybrid Electric Vehicle Tailpipe Emissions Through Supervisory Control Methods," *SAE Intl. Journal of Engines,* vol. 3, pp. 996-1011, 2010.
[10] C. Samaras and K. Meisterling, "Life Cycle Assessment of Greenhouse Gas Emissions from Plug-in Hybrid Vehicles: Implications for Policy," *Environmental Science and Technology,* vol. 42, pp. 3170-3176, 2008.
[11] L. Triger, J. Paterson, and P. Drozdz, "Hybrid Vehicle Engine Size Optimization," Proceedings of *SAE Future Transportation Technology Conference and Exposition, SAE 931793*, San Antonio, Texas, U.S.A., 1993.
[12] S. M. Aceves, J. R. Smith, L. J. Perkins, S. W. Haney, and D. L. Flowers, "Optimization of a CNG Series Hybrid Concept Vehicle," Proceedings of *SAE International Congress and Exposition, SAE 960234*, Detroit, MI, U.S.A., 1996.
[13] T. Moore, "Tools and Strategies for Hybrid-Electric Drivesystem Optimization," Proceedings of *SAE Future Transportation Technology Conference and Exposition, SAE 961660*, Vancouver, Canada, 1996.
[14] U. Zoelch and D. Schroeder, "Dynamic Optimization Method for Design and Rating of the Components of a Hybrid Vehicle," *International Journal of Vehicle Design,* vol. 19, pp. 1-13, 1998.
[15] D. Assanis, G. Delagrammatikas, R. Fellini, Z. Filipi, J. Liedtke, N. Michelena, P. Papalambros, D. Reyes, D. Rosenbaum, A. Sales, and M. Sasena, "An Optimization Approach to Hybrid Electric Propulsion System Design," *Mech. Struct. & Mach.,* vol. 27(4), pp. 393-421, 1999.
[16] R. Fellini, N. Michelena, P. Papalambros, and M. Sasena, "Optimal design of automotive hybrid powertrain systems," Proceedings of *Proceedings First International Symposium on Environmentally Conscious Design and Inverse Manufacturing, 1-3 Feb. 1999*, Los Alamitos, CA, USA, 1999, pp. 400-5.
[17] C. S. N. Shiau, N. Kaushal, C. T. Hendrickson, S. B. Peterson, J. F. Whitacre, and J. J. Michalek, "Optimal Plug-In Hybrid Electric Vehicle Design and Allocation for Minimum Life Cycle Cost, Petroleum Consumption, and Greenhouse Gas Emissions," *Journal of Mechanical Design,* vol. 132, p. 091013 (11), 2010.
[18] P. Pisu and G. Rizzoni, "A Comparative Study of Supervisory Control Strategies for Hybrid Electric Vehicles," *IEEE Transactions on Control Systems Technology,* vol. 15, pp. 506-518, 2007.
[19] J. R. Bumby and I. Forster, "Optimisation and Control of a Hybrid Electric Car," *IEE Proceedings D (Control Theory and Applications),* vol. 134, pp. 373-87, 1987.
[20] Z. S. Filipi, L. S. Louca, B. Daran, C.-C. Lin, U. Yildir, B. Wu, M. Kokkolaras, D. N. Assanis, H. Peng, P. Y. Papalambros, and J. L. J.L. Stein, "Combined Optimization of Design and Power Management of the Hydraulic Hybrid Propulsion System for a 6x6 Medium Truck," *Int. J. of Heavy Vehicle Systems,* vol. 11, Nos 3/4, pp. 372-402, 2004.
[21] "Autonomie," 2011.
[22] S. Songqing and G. G. Wang, "Metamodeling for High Dimensional Simulation-Based Design Problems," *Journal of Mechanical Design,* vol. 132, p. 051009 (11), 2010.
[23] K. J. Astrom and B. Wittenmark, *Adaptive Control: Second Edition*: Dover Publications, 2008.
[24] "Average Carbon Dioxide Emissions Resulting from Gasoline and Diesel Fuel," 2005.
[25] C. L. Weber, P. Jaramillo, J. Marriott, and C. Samaras, "Life cycle assessment and grid electricity: What do we know and what can we know?," *Environmental Science and Technology,* vol. 44(6), pp. 1895-1901, 2010.
[26] "Environmental Assessment of Plug-In Hybrid Electric Vehicles. Volume 1: Nationwide Greenhouse Gas Emissions," 2007.

